scientific reports

Check for updates

OPEN

Research on the material properties of concrete in subway stations after in service for 50 years

Bin Zhang[1], Shaohui He[1]✉, Jianfei Ma[1,2], Jiaxin He[1,2], Yiming Li[1,2] & Jinlei Zheng[1,2]

During the subway operation phase, the performance of concrete materials in subway stations has experienced a series of transformations. This study meticulously investigated the macroscopic and microscopic characteristics of concrete within the Beijing subway structure after 50 years of service. In strict accordance with concrete testing standards, experimental data of 50-year-old concrete were systematically collected to comprehensively analyze the changes in compressive strength, tensile strength, elastic modulus, Poisson's ratio, and bond strength relative to the initial design values. This paper not only detected the condition of concrete aggregates after 50 years of operation but also examined their microstructural states. Moreover, an in-depth study was conducted on the elemental composition and chemical properties of hydrated products in subway station concrete following long-term operation. By delving into the material properties of subway concrete during its long-term operational process, this research offers significant and valuable references for similar underground structures.

Keywords 50-year subway station, Concrete, Mechanical properties, Microscopic characteristics.

The application of concrete dates back to ancient times, embodying a profound historical legacy. Serving as the primary load-bearing material in extant structures, the exploration of concrete durability has persistently occupied a central position in academic research. Presently, the bulk of scholarly investigations predominantly center on the durability of terrestrial concrete structures. Conversely, the durability of subterranean concrete structures remains a relatively under-explored domain, with a paucity of in-depth studies dedicated to this critical aspect of civil engineering.

Owing to the intricate environment and diverse functions of underground concrete structures, stringent requirements are imposed on their bearing capacity and durability, rendering life assessment a challenging task. Ensuring their long-term usability, stability, and safety is of paramount importance[1–5]. Underground concrete structures enhance their mechanical performance by altering material properties, thereby achieving remarkable long-term effects and serviceability[6,7]. Quang Dieu Nguyen[8] explored the exposure of various underground reinforced concrete pipelines to chloride and carbonation environments. The pipelines, with ages spanning from 43 to 70 years, were studied, and it was determined that, based on the minimum concrete protective layer of the steel bars, the service life of these pipelines under the exposure conditions could reach 100 years.

With the continuous transformation of urbanization and population growth, rail transit and underground space will continue to expand, inevitably affecting the operation of underground concrete structures[9–12]. Monitoring and evaluation of underground concrete structures in operation is essential to ensure their long-term availability, stability, and safety as a transportation network to monitor their long-term deterioration over time[13–16].

The long-term performance of underground concrete structures is predominantly governed by the intricate interplay between the structure itself and its surrounding environment. This interaction is instigated by a multitude of factors, encompassing both internal and external, as well as natural and human-induced elements. Owing to the inherent long-term dynamic characteristics of the lining structure and the adjacent rock mass, the equilibrium conditions of underground concrete structures undergo continuous temporal changes[17–23].

Due to the complexity of the underground environment, underground reinforced concrete structures will be affected by complex environments such as groundwater and soil layer loads, thereby affecting the durability of reinforced concrete structures[24–30]. Quang Dieu Nguyen[8] studied the concrete cores from underground reinforced concrete pipes aged 43 to 70 years exposed to chloride salt and carbonation environments, and discussed the durability and service life of the pipes. Pengfei Li[31] proposed using the durability concrete model-complex three-

[1]School of Civil Engineering, Beijing Jiaotong University, Beijing 100044, China. [2]Jianfei Ma, Jiaxin He, Yiming Li & Jinlei Zheng contributed equally to this work. ✉email: heshaohui1122@126.com

dimensional (DuCOM-COM3D) analysis software to conduct numerical simulations of underground culvert projects, investigated the complex mechanical and environmental loads affecting RC structures.

After extended operation, the microscopic characteristics and chemical composition of concrete within underground structures will undergo alterations, thereby influencing the macroscopic mechanical properties of the concrete. Chen Li[32] investigated the chemical and mineralogical transformations in the concrete of underground tunnel structures constructed in China's eastern coastal regions between 1980 and 1996. It was found that the durability of underground concrete structures in Chinese cities has changed following prolonged operation. China's history of constructing underground structures is relatively short. The long-operating subway structure examined in this study is the earliest subway station in China, constructed in 1969. Having been in operation for 50 years, it has endured nearly half a century. The objective of this research is to explore the mechanical properties and microscopic changes of subway concrete stations after five decades of operation.

Currently, research on the concrete performance of subway station structures in long-term operation is scarce. This study endeavors to compare the material mechanical properties and microstructural characteristics of such long-operating subway structures. It does so by referencing the concrete design specifications for subway structure construction in similar years and the material characteristics of 90-day-old C40 concrete.

Background of concrete specimens

The buried depth of the operating subway station is 12 m, and the terrain is flat and stable. The soil layer is mainly divided into clay, sand, and pebbles. There is a groundwater layer within the scope of the subway station, and the chemical composition of the groundwater is not corrosive to the concrete structure. After the apparent state inspection of the station structure, after 50 years of operation of the subway station, there are a few micro-cracks on the surface of the structural concrete, and there are no large cracks in the whole structure. The asphalt waterproof layer is completely protected, and there is no leakage of water in the main structure. Because the subway station structure is less susceptible to environmental factors, this study predominantly focuses on the material properties of the concrete constituting the station structure.

Regarding the design of the underground concrete structure during the construction period, the standard axial compressive strength of the concrete is designed to be 35 MPa, the tensile strength is designed to be 3.0 MPa, and the elastic modulus is designed to be 35 GPa. The cementitious material is mainly ordinary Portland cement. Ribbed steel bars are used as the reinforcement, and the minimum tensile strength is designed to be 500 MPa.

In this study, the concrete of the side wall of the subway station was selected (Fig. 1). In this sampling, the method of combining a water drill and rope saw is used to reduce the disturbance to the sample properties and control the influence of sampling on the bearing capacity of the structure. The sampling process is shown in Fig. 2. After the large volume concrete blocks are processed into cylinders and concrete slabs, the specimens are processed in the specimen processing plant to reduce the test error.

Test size of concrete specimens

In this study, by the Standard for Test Methods of Physical and Mechanical Properties of Concrete (GB/T 50081-2019), the macroscopic mechanical properties of concrete, such as compressive strength, tensile strength, elastic modulus, Poisson's ratio, and the bond strength between concrete and steel bars, were tested. The test specifications strictly adhere to the requirements outlined in the aforementioned standards. For clarity, C100 denotes a cylindrical specimen with dimensions of 100 mm in diameter and 200 mm in height; C150 represents another cylindrical specimen, measuring 150 mm in diameter and 300 mm in height; and P150 refers to a prismatic specimen with dimensions of 150 mm × 150 mm × 300 mm. The bond strength specimens are cubic, with each side measuring 150 mm, and a 500-mm-long steel bar is centrally embedded through the cube. The sampling position and specifications of the microscopic test are shown in Fig. 3.

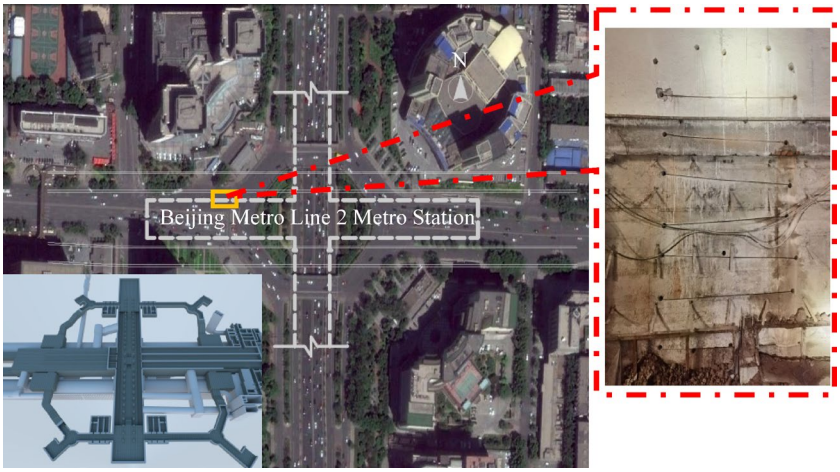

Fig. 1. The surrounding and sampling location of the Beijing Metro Line 2 subway station.

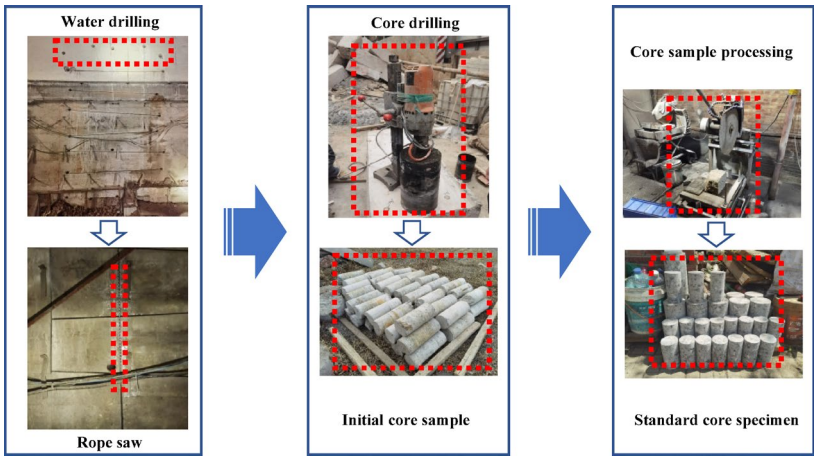

Fig. 2. Sampling flow chart.

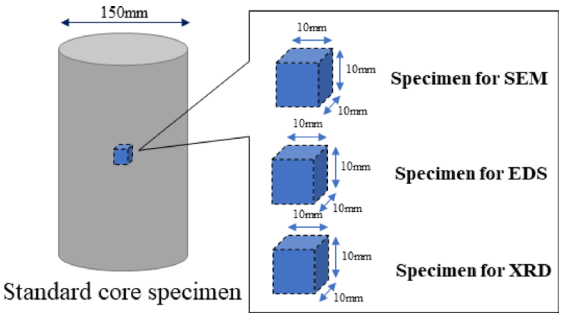

Fig. 3. Micro test sampling position.

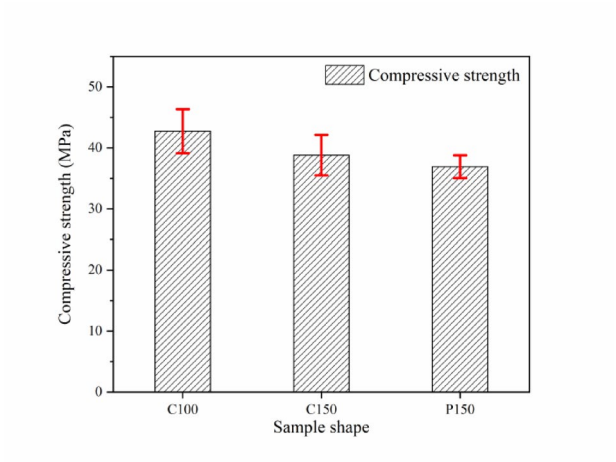

Fig. 4. Compressive strength test results of C100, C150, and P150 samples.

Compressive strength test results of concrete specimens

It can be seen from Fig. 4 that according to the compressive strength test of three groups (three test specimens in each group) with different sizes, the axial compressive strength of C100 is 42.7 MPa, and the standard deviation is 3.6. The axial compressive strength of C150 is 38.8 MPa, and the standard deviation is 3.3. The axial compressive strength of P150 is 36.9 MPa, and the standard deviation is 1.9.

The test results show that the concrete used in the long-term operation station structure conforms to the mechanical characteristics of the compressive strength of ordinary concrete. The discreteness of the compressive strength of C100 and C150 is greater than that of P150.

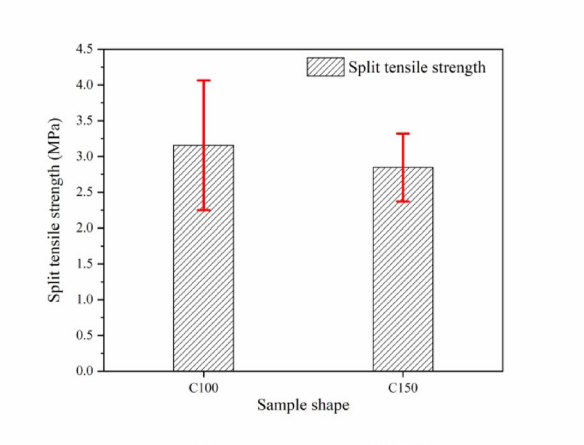

Fig. 5. Splitting tensile strength test results of C100 and C150 samples.

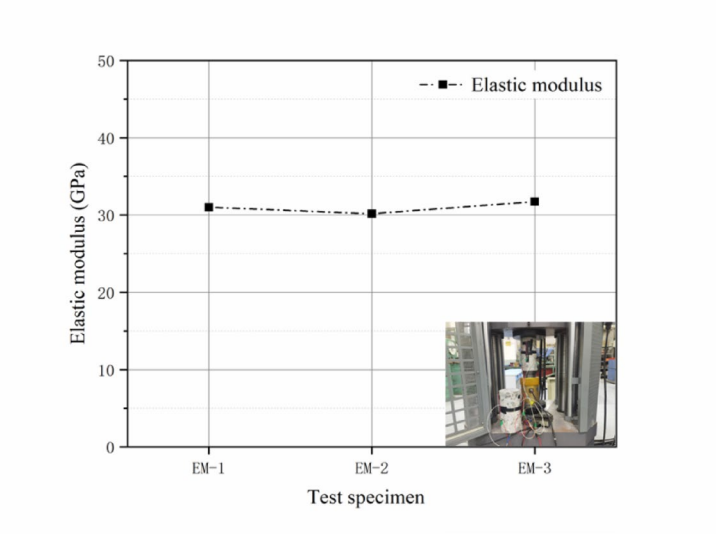

Fig. 6. Static compression elastic modulus test results of C150 samples (EM-1, 2, 3).

According to the specification, the ratio of compressive strength of standard specimens of C100 and C150 is 0.95, and the ratio of compressive strength of standard specimens of C150 and P150 is 1. The ratio of the compressive strength of the test specimen C100 to C150 is 0.91, and the ratio of the compressive strength of the standard specimen C150 to P150 is 1.05.

Splitting tensile strength test results of concrete specimens

It can be seen from Fig. 5 that the splitting tensile strength of C100 is 3.2 MPa, and the standard deviation is 0.9 according to the splitting tensile strength test of two groups (three test specimens in each group) with different sizes. The splitting tensile strength of C150 is 2.8 MPa, and the standard deviation is 0.5.

The tensile strength of C100 is greater than that of C150, which is in line with the mechanical characteristics of the tensile strength of ordinary concrete, and the tensile strength is slightly smaller than the initial tensile strength of concrete. The tensile strength discreteness of C100 is greater than that of C150.

The test results show that the tensile strength of concrete used in the long-term operation station structure is greater than the initial tensile strength of concrete. The tensile strength of C100 is greater than that of C150, and the tensile strength dispersion of C100 is greater than that of C150. The tensile strength of concrete used in the long-term operation station structure is slightly smaller than the initial tensile strength of concrete.

Static compression elastic modulus test results of concrete specimens

It can be seen from Fig. 6 that, according to the measurement results of the three groups (six test specimens in each group) of samples, the static compressive elastic modulus obtained by the C150 cylinder sample is between 30.1 GPa and 31.7 GPa.

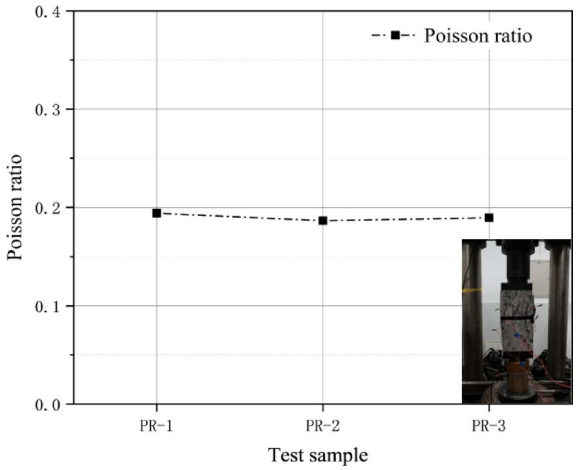

Fig. 7. Poisson's ratio test results of P150 samples (PR-1, 2, 3).

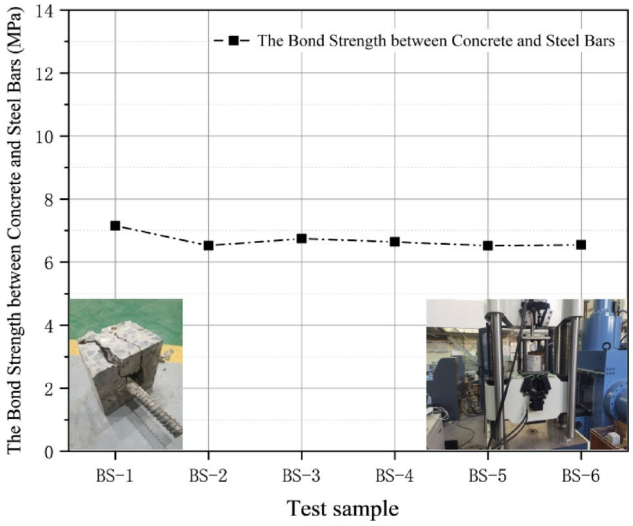

Fig. 8. The test results of bond strength samples (BS-1,2,3,4,5,6).

The elastic modulus is a measure of an object's ability to resist elastic deformation, and the factors that affect the bonding strength of a material can influence the elastic modulus of that material.

The static elastic modulus of concrete reflects the strength of the bond between the cement paste and the aggregates in the concrete[33–35]. When compared with the initial elastic modulus of concrete, the elastic modulus of concrete in the structure of a long-term operational station is slightly lower than the initial elastic modulus of the concrete.

Poisson's Ratio Test Results of Concrete Specimens.

It can be seen from Fig. 7 that, according to the measurement results of the three groups of samples, the Poisson's ratio value of the long-term operation station structure concrete measured by the P150 prism sample is about 0.2.

Poisson's ratio, an elastic constant, characterizes the transverse deformation of materials and is expressed as a dimensionless quantity obtained through experimental measurements. Experimental evidence confirms that the elastic deformation properties of concrete utilized in long-term operational station structures align closely with those of ordinary concrete[36–39].

Bond strength test results of concrete specimens

According to the test phenomenon and Fig. 8, it can be seen that the bonding strength between the concrete and steel bar of the long-term operation station structure is about 6.69 MPa.

According to the load-displacement curve of the bond strength, it can be seen that the failure mode of the pull-out test is splitting failure. Different from the pull-out failure of steel bars, the splitting failure is more sudden, the early deformation is slow, and the later deformation is faster[40].

The steel bar used in the bonding test is a ribbed steel bar. Compared with a round steel bar, it has a larger bonding surface area and exhibits mechanical interlocking[41]. Owing to the complete hydration reaction of cement in the concrete, the strength of the concrete increases. As a result, the bonding force of the concrete becomes stronger than that in the early construction stage, and the interfacial bonding state between the steel bar and the concrete is more favorable[42–44].

Comparison between material test results and design values of concrete

Material test	Design values	Test results
Compressive strength	35 MPa	38.8 MPa
Tensile strength	3.0 MPa	2.8 MPa
Elastic modulus	35 GPa	30.1–31.7 GPa
Poisson 's ratio	0.2	0.2

Test results of optical observation of minerals

The optical microscope was used to observe the concrete samples of the long-running station structure, and the microscopic photos were taken under the orthogonal microscope.

Through optical microscope imaging observation (Fig. 9), the composition and state of aggregate in concrete are as follows.

The aggregate particle size is generally between 0.5 cm and 3 cm, and the particle size distribution is relatively uniform, mainly composed of broken gravel and pebbles. The aggregate composition is mainly two kinds, one is rock debris, and the other is single mineral debris. The mineral debris is mainly quartz and feldspar, which account for more than 95% of the total mineral debris, and a small amount of mica and hornblende. Between the aggregates are cement hydration products.

According to the observation, both rock debris and mineral debris are relatively fresh, and there is no obvious weathering phenomenon. In particular, mica and hornblende with weak weathering resistance have not yet been seen in traces of weathering.

Test results of SEM

Through the scanning electron microscope (SEM), the cement microstructure of the long-term operation station structure concrete and the 90-day-old C40 concrete were observed and compared to study the difference between the microstructure of the super-long-age concrete and the short-age concrete. C40 concrete is a type of cast-in-place concrete which is prepared by blending Portland cement, aggregate, fly ash, admixtures, and other raw materials in a specific ratio.

According to the observation results (Fig. 10), it can be seen that the cement hydration products in the concrete of the existing underground station structure are dense, and the degree of hydration is almost complete. There are no obvious micro-cracks, and there are some holes formed in the hydration process. Due to incomplete hydration, the microstructure of cement in 90-day C40 concrete contains more microcracks than that of existing structural concrete.

The cement hydration products of the existing underground station structure concrete and the microstructure of the aggregate interface are compared as follows:

It can be seen from the above observation results that there are microcracks along the aggregate surface at the interface between the cement and the aggregate of the existing underground station structure concrete (Fig. 11).

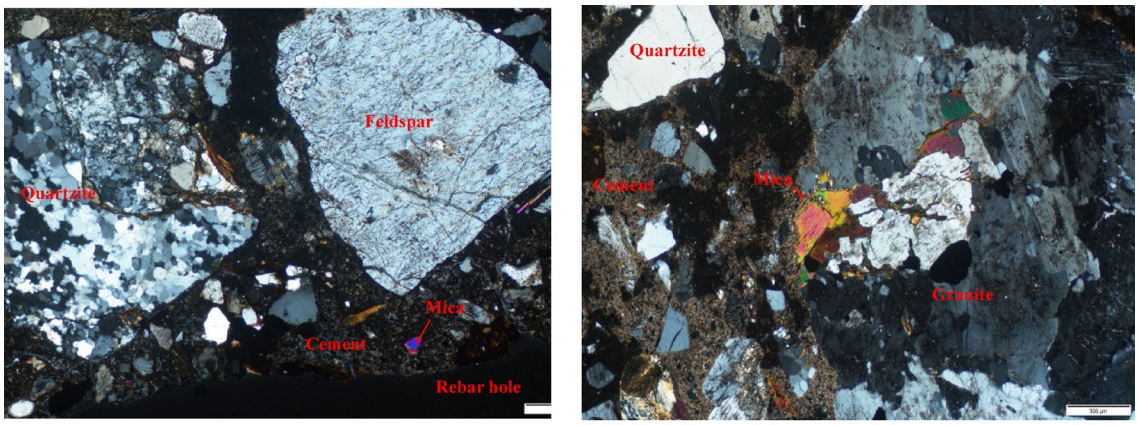

Fig. 9. (**a**) Optical microscope imaging (with rebar holes); (**b**) Optical microscope imaging (in cement).

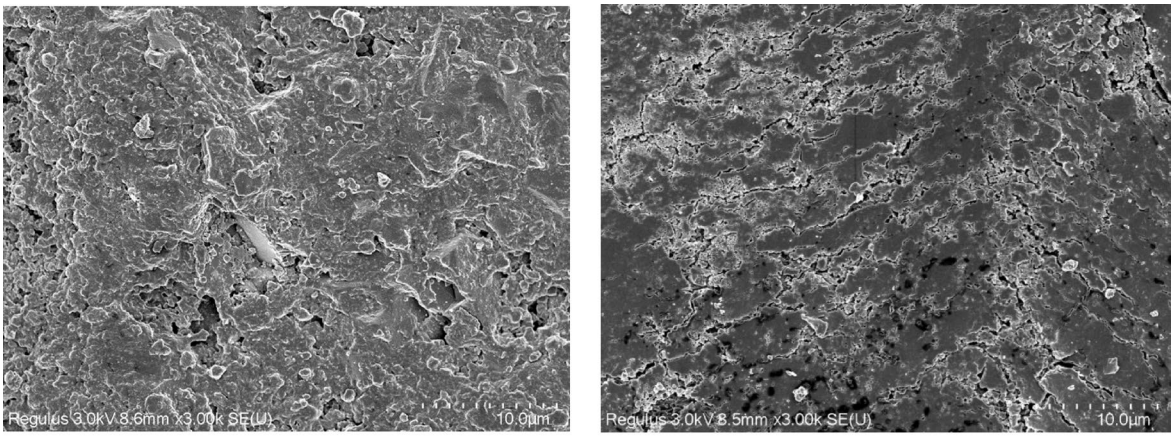

(a) **(b)**

Fig. 10. (**a**) Microstructure of hydrated cement paste in the existing underground station structure; (**b**) Microstructure of cement in the 90-day-old C40 concrete.

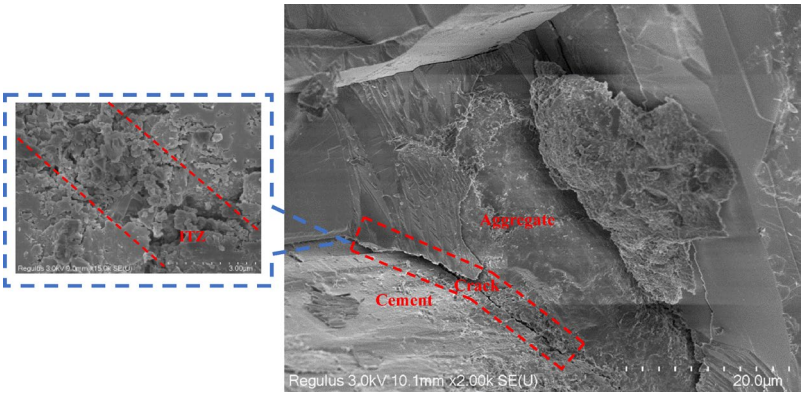

Fig. 11. Microstructure of the interface between hydrated cement paste and aggregate of the existing underground station structure concrete.

There exists an uncompacted area in the interfacial transition zone between the aggregate and the cement paste. In the early stage of the station construction, the concrete was mixed on-site.

During the mixing process, the non-uniform dispersion of cement particles and inadequate wetting of aggregates render the interface highly susceptible to segregation, as documented in references[45,46]. As cement hydration progresses over an extended period, the bonding capacity of the cement paste is enhanced. Nevertheless, the presence of the aggregate interface inevitably diminishes the interfacial bond strength, facilitating the initiation and propagation of microcracks[47]. These microcracks compromise the bond strength within the interfacial transition zone (ITZ) between aggregates and cement paste, thereby exerting a significant influence on the overall mechanical performance of concrete, as evidenced by studies[46,48–50].

Test results of EDS

The EDS test used the geological glass processed by the existing underground station structure concrete sample. The ion distribution of hydrated cement paste in the concrete of the existing underground station structure was observed by EDS to study the element composition of the ultra-long-age concrete.

Based on the Energy Dispersive Spectroscopy (EDS) test results, the elemental components of the hydrated phases in the existing concrete predominantly consist of calcium, aluminum, silicon, oxygen, and iron. These components exhibit a strong resemblance to those of the hydrated phases in Portland cement, as illustrated in Figs. 12, 13 and 14. Since the cement hydration reaction is complete, according to the element ratio of cement hydrate, the hydration products are determined to be hydrated calcium silicate, hydrated calcium aluminate, and hydrated iron calcium aluminate.

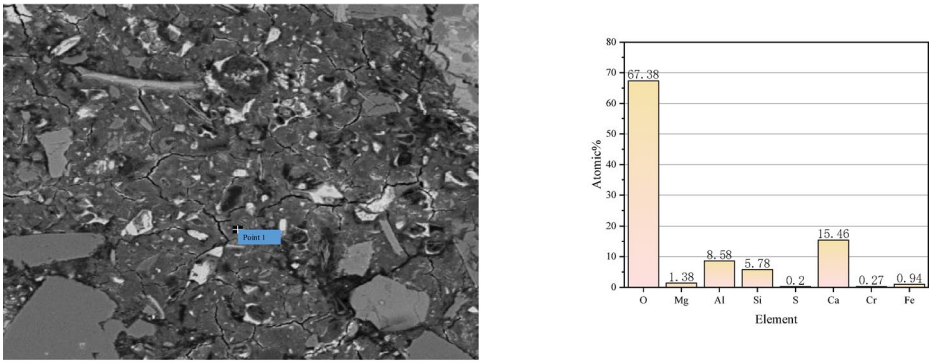

(a) (b)

Fig. 12. (**a**) The concrete slice point 1 position; (**b**) Element composition of concrete slice point 1 position.

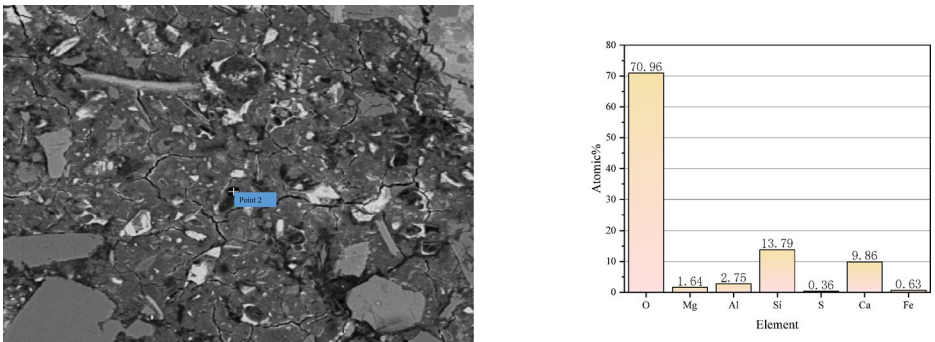

(a) (b)

Fig. 13. (**a**) The concrete slice point 2 position; (**b**) Element composition of concrete slice point 3 position.

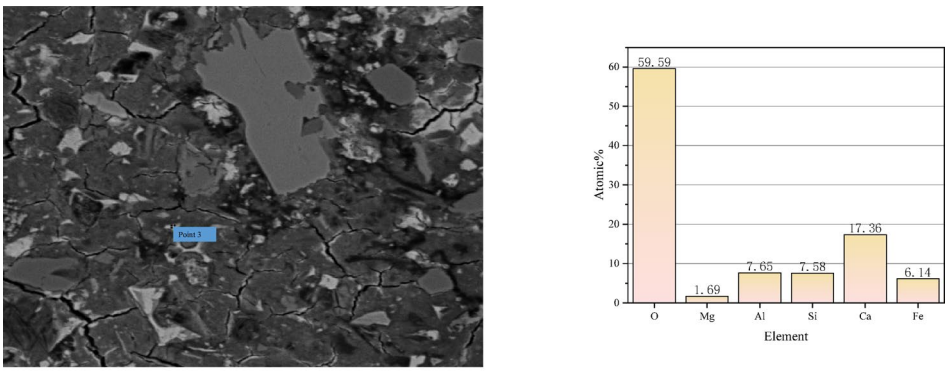

(a) (b)

Fig. 14. (**a**) The concrete slice point 3 position; (**b**) Element composition of concrete slice point 3 position.

Microscopic test results of XRD

The XRD test uses the samples processed by the existing underground station structure concrete. The mineral composition of hydrated cement paste in the existing underground station structure concrete was detected by XRD test.

Researchers studied the crystal phases and mineral contents of concrete samples under the conditions of 50 years of service using XRD (X-ray diffraction) analysis, with a special emphasis on the phases of calcite and silica[51,52]. Figures 15 and 16 display the X-ray diffraction (XRD) curves of Sample 1 and Sample 2. As the

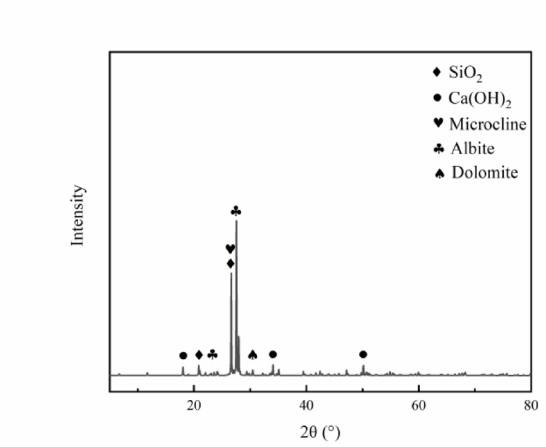

Fig. 15. Composition of compounds in concrete sample 1.

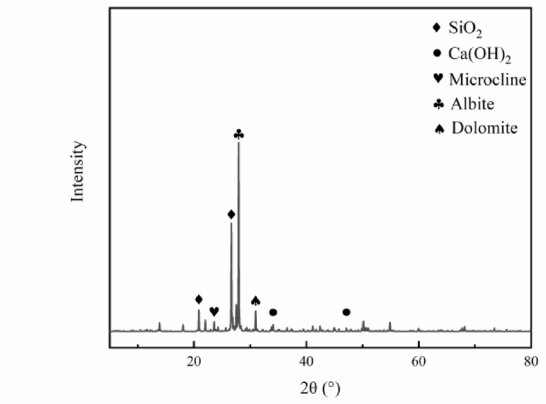

Fig. 16. Composition of compounds in concrete sample 2.

composition of the concrete is mainly aggregate, most of the diffraction peaks of the crystalline phases (both anhydrous and hydrated compounds) could not be identified. The diffraction peaks of quartz and the hydration product $Ca(OH)_2$ in the sample composition are identifiable. No diffraction peaks associated with calcite were observed in the X-ray diffraction pattern. This observation may imply that under the conditions of 50 years, only a small quantity of $Ca(OH)_2$ crystals were detected by XRD, indicating that the internal environment of the sample remains alkaline and no carbonation reaction has taken place[53–55]. The concrete inside the long-term operating station has not experienced carbonation[56]. Minerals such as C_2S, C_2S, C_2A, and C_4AF were not detected in the analysis, suggesting that the Portland cement has mostly hydrated after 50 years. This could be attributed to the relatively stable environment of the long-term subway station structure and the pozzolanic reactions[47,57–59].

Conclusions

After 50 years of operation, an existing underground station was studied to evaluate its current concrete mechanical properties and microstructural characteristics, leading to the following conclusions:

1. The aggregate morphology of the concrete in the existing underground station structure remains fresh after 50 years of operation, with no significant signs of weathering. The reinforcement has not corroded, and the internal concrete structure remains undamaged.
2. The cement in the underground station concrete is well-hydrated with no carbonation. Yet, microcracks around aggregates, along with this enhanced cohesion, jointly impact concrete's mechanical properties.
3. After 50 years of operation, the mechanical properties of the existing underground station concrete have changed. These changes are primarily attributed to the complete hydration of the cement and the presence of microcracks at the cement-aggregate interface.

4. The observed dispersion in specimen strength can be predominantly attributed to the stochastic distribution of microcrack locations, lengths, and densities within the concrete matrix.
5. This study provides material strength for numerical model research in subway engineering and lays a foundation for the subsequent study of the durability and toughness of existing subways.

Data availability

All data generated or analysed during this study are included in this published article.

Received: 13 May 2025; Accepted: 10 July 2025
Published online: 16 July 2025

References

1. Kim, M. S. & Lee, S. S. Design study of steel fibre reinforced concrete shaft lining for swelling ground in toronto, Canada. *Appl. Sci.* **11**, 3490. https://doi.org/10.3390/app11083490 (2021).
2. Ratnika, L., Gaile, L. & Vatin, N. Impact of groundwater level change on natural frequencies of RC buildings. *Buildings*. **11**, 265. https://doi.org/10.3390/buildings11070265 (2021).
3. Han, S. J., Ishida, T. & Tsuchiya, S. Numerical evaluation on the effect of rebar corrosion on long-term structural behavior of underground RC culverts. *Structures*. **48**, 1920–1931. https://doi.org/10.1016/j.istruc.2023.01.081 (2023).
4. Lu, F. et al. Safety evaluation of plain concrete lining considering deterioration and aerodynamic effects. *Sustainability*. **15**, 7170. https://doi.org/10.3390/su15097170 (2023).
5. Afshani, A., Li, W., Oka, S., Itoh, Y. & Akagi, H. Study of the long-term behavior of segmented tunnels in cohesive soil based on the circumferential joint opening. *Tunn. Undergr. Space Technol.* **120**, 104210. https://doi.org/10.1016/j.tust.2021.104210 (2022).
6. Hossain, M. S., Han, S., Kim, S. K. & Yun, K. K. Long-term effect of accelerator content on flexural toughness of steel fiber reinforced shotcrete for tunnel construction. *Case Stud. Constr. Mater.* **15**, e00706. https://doi.org/10.1016/j.cscm.2021.e00706 (2021).
7. Vogel, F., Sovják, R. & Pešková, Š. Static response of double shell concrete lining with a spray-applied waterproofing membrane. *Tunn. Undergr. Space Technol.* **68**, 106–112. https://doi.org/10.1016/j.tust.2017.05.022 (2017).
8. Nguyen, Q. D. & Castel, A. Long-term durability of underground reinforced concrete pipes in natural chloride and carbonation environments. *Constr. Build. Mater.* **394**, 132230. https://doi.org/10.1016/j.conbuildmat.2023.132230 (2023).
9. Qiu, J. et al. Investigating the long-term settlement of a tunnel built over improved loessial foundation soil using jet grouting technique. *J. Perform. Constr. Facil.*
10. Wang, F. et al. Numerical simulation study on lining damage of shield tunnel under train load. *Sustainability*. **14**, 14018. https://doi.org/10.3390/su142114018 (2022).
11. Yi, H. et al. Influence of long-term dynamic load induced by high-speed trains on the accumulative deformation of shallow buried tunnel linings. *Tunn. Undergr. Space Technol.* **84**, 166–176. https://doi.org/10.1016/j.tust.2018.11.005 (2019).
12. Soga, K., Laver, R. G. & Li, Z. Long-term tunnel behaviour and ground movements after tunnelling in clayey soils. *Undergr. Space*. **2**, 149–167. https://doi.org/10.1016/j.undsp.2017.08.001 (2017).
13. Wang, C., Friedman, M. & Li, Z. Monitoring and assessment of a cross-passage twin tunnel long-term performance using wireless sensor network. *Can. Geotech. J.* **60**, 1140–1160. https://doi.org/10.1139/cgj-2022-0224 (2023).
14. Maes, K., Salens, W., Feremans, G., Segher, K. & François, S. Anomaly detection in long-term tunnel deformation monitoring. *Eng. Struct.* **250**, 113383. https://doi.org/10.1016/j.engstruct.2021.113383 (2022).
15. Tang, C., He, S. Y. & Zhou, W. H. Settlement-based framework for long-term serviceability assessment of immersed tunnels. *Reliab. Eng. Syst. Saf.* **228**, 108801. https://doi.org/10.1016/j.ress.2022.108801 (2022).
16. Tuchiya, Y., Kurakawa, T., Matsunaga, T. & Kudo, T. Research on the long-term behaviour and evaluation of lining concrete of the Seikan tunnel. *Soils Found.* **49**, 969–980. https://doi.org/10.3208/sandf.49.969 (2009).
17. Sandrone, F. & Labiouse, V. Analysis of the evolution of road tunnels equilibrium conditions with a convergence–confinement approach. *Rock. Mech. Rock. Eng.* **43**, 201–218. https://doi.org/10.1007/s00603-009-0056-y (2010).
18. Zhang, Z., Gong, R., Zhang, H. & He, W. The sustainability performance of reinforced concrete structures in tunnel lining induced by long-term coastal environment. *Sustainability*. **12**, 3946. https://doi.org/10.3390/su12103946 (2020).
19. Wang, C., Friedman, M., Wu, W., Zhang, D. & Li, Z. Hydraulic influences on the long-term performance of tunnels: A review. *Transp. Geotech.* **48**, 101329. https://doi.org/10.1016/j.trgeo.2024.101329 (2024).
20. Kovačević, M. S., Bačić, M., Gavin, K. & Stipanović, I. Assessment of long-term deformation of a tunnel in soft rock by utilizing particle swarm optimized neural network. *Tunn. Undergr. Space Technol.* **110**, 103838. https://doi.org/10.1016/j.tust.2021.103838 (2021).
21. Liu, W. et al. Long-term stress monitoring and in-service durability evaluation of a large-span tunnel in squeezing rock. *Tunn. Undergr. Space Technol.* **127**, 104611. https://doi.org/10.1016/j.tust.2022.104611 (2022).
22. Vu, M. N. & Broere, W. Structural design model for tunnels in soft soils: from construction stages to the long-term. *Tunn. Undergr. Space Technol.* **78**, 16–26. https://doi.org/10.1016/j.tust.2018.04.017 (2018).
23. Wang, B., Zhang, Z., He, C. & Zheng, H. Implementation of a long-term monitoring approach for the operational safety of highway tunnel structures in a severely seismic area of China.
24. Xie, Y. et al. Life prediction of underground structure by sulfate corrosion using Harris Hawks optimizing genetic programming. *Eng. Appl. Artif. Intell.* **115**, 105190. https://doi.org/10.1016/j.engappai.2022.105190 (2022).
25. He, Z. S., Supasit, S., Akiyama, M. & Frangopol, D. M. Life-cycle reliability-based design and reliability updating of reinforced concrete shield tunnels in coastal regions. *Struct. Infrastruct. Eng.* **16**, 726–737. https://doi.org/10.1080/15732479.2019.1674343 (2020).
26. Chen, J., Song, X., Zhao, T. & Tian, L. Service life prediction of lining concrete of subsea tunnel under combined compressive load and carbonation. *J. Wuhan Univ. Technol. -Mat Sci. Edit.* **25**, 1061–1064. https://doi.org/10.1007/s11595-010-0150-8 (2010).
27. Kwon, S. J., Lee, B. J. & Kim, Y. Y. Concrete mix design for service life of RC structures under carbonation using genetic algorithm. *Adv. Mater. Sci. Eng.* **2014**, 1–13. https://doi.org/10.1155/2014/653753 (2014).
28. Ji, G. M., Kanstad, T. & Bjøntegaard, Ø. Crack risk evaluation of submerged concrete tunnel during hardening phase. *Adv. Civ. Eng.* **2018**, 7354025 https://doi.org/10.1155/2018/7354025 (2018).
29. Yang, W., Baji, H. & Li, C. Q. Time-dependent reliability method for service life prediction of reinforced concrete shield metro tunnels. *Struct. Infrastruct. Eng.* **14**, 1095–1107. https://doi.org/10.1080/15732479.2017.1401094 (2018).
30. Cassiani, J. D., Dugarte, M., Arteta, C. A. & Kessler, S. Durability assessment of a tunnel structure with two-sided chloride ingress—A case study located in a tropical environment. *Struct. Concrete.* **23**, 739–752. https://doi.org/10.1002/suco.202100550 (2022).
31. Li, P., Wang, H., Nie, D., Wang, D. & Wang, C. A method to analyze the long-term durability performance of underground reinforced concrete culvert structures under coupled mechanical and environmental loads. *J. Intell. Constr.* **1**, 1–17. https://doi.org/10.26599/JIC.2023.9180011 (2023).

32. Li, C., Wu, M., Chen, Q. & Jiang, Z. Chemical and mineralogical alterations of concrete subjected to chemical attacks in complex underground tunnel environments during 20–36 years. *Cem. Concr. Compos.* **86**, 139–159. https://doi.org/10.1016/j.cemconcomp.2017.11.007 (2018).
33. Hashin, Z. & Monteiro, P. J. M. An inverse method to determine the elastic properties of the interphase between the aggregate and the cement paste. *Cement Concr. Res.* (2002).
34. Rangaraju, P. R., Olek, J. & Diamond, S. An investigation into the influence of inter-aggregate spacing and the extent of the ITZ on properties of Portland cement concretes. *Cem. Concr. Res.* **40**, 1601–1608. https://doi.org/10.1016/j.cemconres.2010.07.002 (2010).
35. Zheng, J. & An, N-L. Spherical inclusion model for predicting the elastic moduli of concrete with inhomogeneous ITZ (2012).
36. Thomas, R. J. & Peethamparan, S. Alkali-Activated Concrete: Engineering properties and Stress–Strain behavior. *Constr. Build. Mater.* **93**, 49–56. https://doi.org/10.1016/j.conbuildmat.2015.04.039 (2015).
37. Barnes, C. L. & Trottier, J. F. Hybrid analysis of surface wavefield data from Portland cement and asphalt concrete plates. *NDT E Int.* **42**, 106–112. https://doi.org/10.1016/j.ndteint.2008.10.003 (2009).
38. Liu, Z., Asce, S. M. & Cai, C. S. Experimental study of the geopolymeric recycled aggregate concrete. *J. Mater. Civ. Eng.*
39. Palmquist, S. M., Jansen, D. C. & Swan, C. W. Compressive behavior of concrete with vitrified soil aggregate. *J. Mater. Civ. Eng.* **13**, 389–394. https://doi.org/10.1061/(ASCE)0899-1561(2001)13:5(389) (2001).
40. Cui, Y. et al. Effect of corrosion on the bond behavior of steel-reinforced. *Alkali-Activ. Slag Concrete Mater.* **16**, 2262. https://doi.org/10.3390/ma16062262 (2023).
41. Wang, H. Influencing aspects and mechanisms of steel bar reinforcement on shrinkage and cracking of cement-based materials: A review. *J. Build. Eng.* (2023).
42. Vembu, P. R. S. & Ammasi, A. K. A Comprehensive review on the factors affecting bond strength in concrete (2023).
43. Li, W., Shumuye, E. D., Shiying, T., Wang, Z. & Zerfu, K. Eco-friendly fibre reinforced geopolymer concrete: A critical review on the microstructure and long-term durability properties. *Case Stud. Constr. Mater.* **16**, e00894. https://doi.org/10.1016/j.cscm.2022.e00894 (2022).
44. Hosseini, S. A. The effect of fly ash on the bond strength of steel reinforcement and concrete. *Iran. J. Sci. Technol.* (2022).
45. Scrivener, K. L., Crumbie, A. K. & Laugesen, P. The interfacial transition zone (ITZ) between cement paste and aggregate in concrete. *Interface Sci.* **12**, 411–421. https://doi.org/10.1023/B:INTS.0000042339.92990.4c (2004).
46. Huang, L., Yu, L., Zhang, H. & Yang, Z. Composition and microstructure of 50-Year lightweight aggregate concrete (LWAC) from Nanjing Yangtze river Bridge (NYRB). *Constr. Build. Mater.* **216**, 390–404. https://doi.org/10.1016/j.conbuildmat.2019.05.015 (2019).
47. Zhang, J. & Lv, T. Hydration and durability of Low-Heat cementitious composites for dam concrete: thermodynamic modeling and experiments. *Front. Mater.* **10**, 1120520. https://doi.org/10.3389/fmats.2023.1120520 (2023).
48. Xu, L. et al. Investigations on micro-mechanical properties of the ITZs between recycled aggregates and recycled cement paste. *Constr. Build. Mater.* **450**, 138640. https://doi.org/10.1016/j.conbuildmat.2024.138640 (2024).
49. Gao, Y., De Schutter, G., Ye, G., Tan, Z. & Wu, K. The ITZ microstructure, thickness and porosity in blended cementitious composite: effects of curing age, water to binder ratio and aggregate content. *Compos. Part. B: Eng.* **60**, 1–13. https://doi.org/10.1016/j.compositesb.2013.12.021 (2014).
50. Wang, Z. et al. Long-Term properties and microstructure change of engineered cementitious composites subjected to high sulfate coal mine water in Drying-Wetting cycles. *Mater. Des.* **203**, 109610. https://doi.org/10.1016/j.matdes.2021.109610 (2021).
51. Dollimore, D., Lerdkanchanaporn, S., Gupta, J. D. & Nippani, S. An examination of recycled Portland cement concrete rich in dolomite and low in calcite obtained from various locations in Ohio. *Thermochim. Acta*. 367–368. https://doi.org/10.1016/S0040-6031(00)00664-X (2001).
52. Qing, Y., Huxing, C., Yuqing, W., Shangxian, W. & Zonghan, L. Effect of MgO and gypsum content on long-term expansion of low heat Portland slag cement with slight expansion. *Cem. Concr. Compos.* **26**, 331–337. https://doi.org/10.1016/S0958-9465(02)00145-2 (2004).
53. Pizzol, V. D. et al. Mineralogical and microstructural changes promoted by accelerated carbonation and ageing cycles of hybrid fiber–cement composites. *Constr. Build. Mater.* **68**, 750–756. https://doi.org/10.1016/j.conbuildmat.2014.06.055 (2014).
54. Kwon, S. J., Lee, H. S., Karthick, S., Saraswathy, V. & Yang, H. M. Long-term corrosion performance of blended cement concrete in the marine environment—a real-time study. *Constr. Build. Mater.* **154**, 349–360. https://doi.org/10.1016/j.conbuildmat.2017.07.237 (2017).
55. Zhang, M., Zunino, F., Yang, L., Wang, F. & Scrivener, K. Understanding the negative effects of alkalis on long-term strength of Portland cement. *Cem. Concr. Res.* **174**, 107348. https://doi.org/10.1016/j.cemconres.2023.107348 (2023).
56. Ruviaro, A. S. et al. Long-term effect of recycled aggregate on microstructure, mechanical properties, and CO2 sequestration of rendering mortars. *Constr. Build. Mater.* **321**, 126357. https://doi.org/10.1016/j.conbuildmat.2022.126357 (2022).
57. Luke, K. & Lachowski, E. Internal composition of 20-year-old fly ash and slag-blended ordinary Portland cement pastes. *J. Am. Ceram. Soc.* **91**. (2008).
58. Buchwald, A., Vanooteghem, M., Gruyaert, E., Hilbig, H. & De Belie, N. Purdocement: application of alkali-activated slag cement in Belgium in the 1950s. *Mater. Struct.* **48**, 501–511. https://doi.org/10.1617/s11527-013-0200-8 (2015).
59. Sivakumar, N. K., Muthusamy, N., Periasamy, S. & Manivannan, V. R. Reinventing Concrete: Exploring strength and durability with Portland slag cement. *Matéria (Rio J).* **29**, e20240156. https://doi.org/10.1590/1517-7076-rmat-2024-0156 (2024).

Acknowledgements

The authors would like to thank Jie Li of University of Science and Technology Beijing for his assistance with the experimental test.

Author contributions

S.H. and B.Z. conceived the experiment(s). B.Z., and J.Z. conducted the experiment(s), and B.Z., Y.L., J.H., J.M. performed statistical analysis and figure generation. All authors reviewed the manuscript.

Declarations

Competing interests

The authors declare no competing interests.

Additional information

Correspondence and requests for materials should be addressed to S.H.